Dilatancy in Slow Granular Flows

Alexandre J. Kabla*
Department of Engineering, University of Cambridge, Trumpington Street, Cambridge CB2 1PZ, United Kingdom

Tim J. Senden
Department of Applied Mathematics, Research School of Physics and Engineering, The Australian National University, Canberra, 0200 Australia

(Received 8 October 2008; published 3 June 2009)

When walking on wet sand, each footstep leaves behind a temporarily dry impression. This counterintuitive observation is the most common illustration of the Reynolds principle of dilatancy: that is, a granular packing tends to expand as it is deformed, therefore increasing the amount of porous space. Although widely called upon in areas such as soil mechanics and geotechnics, a deeper understanding of this principle is constrained by the lack of analytical tools to study this behavior. Using x-ray radiography, we track a broad variety of granular flow profiles and quantify their intrinsic dilatancy behavior. These measurements frame Reynolds dilatancy as a kinematic process. Closer inspection demonstrates, however, the practical importance of flow induced compaction which competes with dilatancy, leading more complex flow properties than expected.

DOI: 10.1103/PhysRevLett.102.228301 PACS numbers: 83.80.Fg, 47.57.Gc, 83.50.−v

The impact of granular flows on our daily lives is often understated, yet grains represent the second most common material displaced by humans. Consideration of just a few of these activities such as the efficient transport of grain, the optimal compaction of building materials and the prediction of rock slides demonstrates the strikingly complex behavior of these materials. Many of these global phenomena have been studied in detail; to mention a few, a finite angle of repose and avalanching [1], spontaneous jamming [2], dilatancy [3], compaction [4], shear banding [5], or grain segregation [6]. However, theoretical advances are hampered by fundamental problems such as history dependent effects or heterogeneous flow profiles, stressing the need for new tools to define and measure intrinsic local parameters. Tackling such issues in granular systems represents an important step towards a general understanding of the dynamics and rheology of athermal and soft glassy systems [7].

The phenomenon of dilatancy [3] corresponds to the decrease of a grain pile's density upon shear. The intuitive interpretation is that free volume is required for grains to rearrange. This property is typically quantified at small deformation by shearing a sample and measuring the ratio between imposed boundary displacement and resulting thickness change at constant pressure [8]. However, efficient flow predictions rely on the determination and testing of constitutive equations valid up to large deformations, where flow profiles need to be characterized. Along that line, dilatancy during shear band formation has been recently highlighted [9,10], but a general framework for dilatancy in granular flows is still needed.

We introduce here an experimental approach which combines real time x-ray radiography and DIC (Digital Image Correlation) techniques to locally quantify both density variations and strain tensors in a range of 3D granular flows. In particular, we have studied gravity flows and forced shear flows. Flows are generated in rectangular containers, typically 5 cm wide, 3 cm thick, 20 cm high and filled with millimetric grains. In the forced shear experiment, we use a particular geometry where a rigid bracket moves slowly upward while a small wall prevents grains from falling below the bracket [Fig. 1(a)]. The bracket and the opposite wall are fully covered by bound grains to maximize friction. As discussed later, the complexity of the resulting flow profile is a key element to probe the generality of our observations. The gravity driven experiment consists of a large smooth wall moving upward in a similarly dimensioned container as before [Fig. 1(b)]. Withdrawing the partition progressively frees space below it such that grains are free to flow into the void. Unlike the first configuration, the grains freely slip against the walls. In both situations, flows are invariant along the cell thickness and studied in the quasistatic limit, the walls being moved incrementally at speeds of about 0.1 $\mathrm{mm\,s^{-1}}$, i.e., one grain every ten seconds.

X-Ray absorption is classically used to quantify minute density variations in 3D piles; for instance, to study the onset of shear banding [11] or compaction [12]. Recent progress in real time x-ray imaging allows now to study more dynamic processes such as preavalanche dynamics [13]. We use here the same setup as in [13] [Fig. 1(c)] to acquire series of x-ray images while grains are flowing. The intensity in a radiograph takes the following form:

$$I(x, y, t) = I_0(x, y, t) \exp\left(-\frac{L_g(x, y, t)}{\lambda_g}\right) \qquad (1)$$

where $L_g(x, y, t)$ represents the local length of grain crossed by the x-ray beam at the coordinates (x, y)

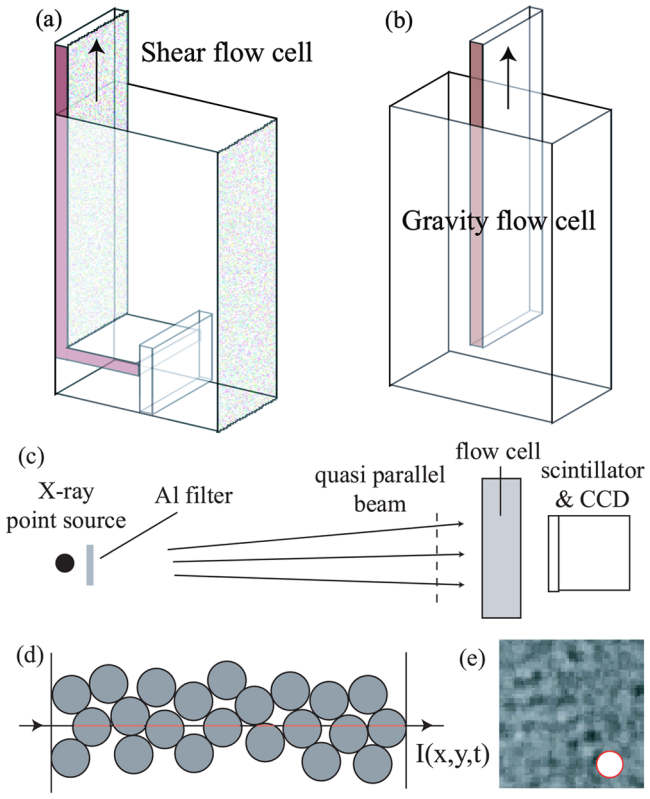

FIG. 1 (color online). (a) Shear flow cell. (b) Gravity flow cell. Moving parts, shown with darker sides, move over 3 cm (20–50 grains) for (a) and 8 cm (50–100 grains) for (b). The beam enters the chambers from the front side. (c) X-ray images acquisition setup. Source settings: 80 kV and 150 μA. A 2 mm Al filter reduces beam hardening. The cell is 2.3 m away from the source, ensuring a quasiparallel beam. (d) Illustration of the path of an x-ray and (e) resulting material length image $L_g(x, y)$. Circle indicates the grain size.

[Fig. 1(d)], λ_g corresponds to the absorption coefficient of the grain material (assuming the absorption is uniform in the beam spectrum); it is measured independently. $I_0(x, y, t)$ accounts for the angular variation in x-ray source intensity, the source temporal intensity fluctuations, as well as the absorption of the container itself and variations in detector sensitivity across the face of the detector. To determine $I_0(x, y, t)$, we record radiographs $I_{wg}(x, y, t) = \alpha(t) I_0(x, y, t)$ of an empty container in exactly the same geometrical configuration. The scalar $\alpha(t)$ is due to random intensity fluctuations of the source; we use a region S without grain, i.e., where $I(x, y, t) = I_0(x, y, t)$, to quantify it: $\alpha(t) = \langle I_{wg}(x, y, t)/I(x, y, t)\rangle_S$. The local grain thickness is then provided by

$$L_g(x, y, t) = \lambda_g \ln\left(\frac{I_{wg}(x, y, t)}{\alpha(t) I(x, y, t)}\right). \quad (2)$$

The average grain density over an arbitrary domain D which spans the sample thickness is directly obtained from $\langle \rho(x, y, t)\rangle_D = \langle L_g(x, y, t)\rangle_D / L$ where L is the gap between the front and rear walls of the container.

DIC is now a standard tool to quantify strain fields in complex or composite media such as fiber structures [14], biological tissues [15], and granular materials [9]. Here, we use the fact that the density images exhibit a noise pattern at the grain scale [Fig. 1(e)] to reconstruct material point trajectories during whole experiments. This spatial pattern is a signature of the local 3D structure of the packing and is advected with the grains, although it progressively evolves with the strain. In practice, displacement increments around half a grain diameter and total pile thickness of up to 50 grains provide robust measurement conditions for cross-correlation methods.

Using the flow trajectories, we determine the evolution of local domains arranged on a grid, and quantify for each of them, at each instant, the local density and total strain from the initial state. Figure 2 shows the typical flow and density profiles for both chambers. The initial configuration was prepared by slowly pouring grains into the container while mechanically tapping the cell, providing initial packing fractions about 0.64 with a suitable homogeneity across the cell. Both experiments exhibit strong correlations between the local deformation and the packing fraction variation. The local shear (deviatoric component of the 2D strain tensor) is accounted for by a scalar $s = |\lambda_1 - \lambda_2|/2$ where λ_1 and λ_2 are the eigenvalues of the logarithmic strain tensor for finite deformations [16]. Figure 3 shows in a scatter plot the local values of the packing fraction and shear s for a broad range of different shear histories and stress states. The data allow us to define a characteristic shear strain s_c after which the steady state (loose limit) is locally reached. An empirical exponential relationship between the local strain and density, as suggested in [17], is consistent with our results:

$$\rho(\epsilon) = \rho_{\min} + (\rho_{\max} - \rho_{\min}) \exp(-s/s_c). \quad (3)$$

The pile response remains qualitatively unchanged with rougher grain shapes and/or larger polydispersity [Fig. 4(a) and 4(b)], the value of critical deformation s_c being systematically about 0.2–0.3. These results indicate that Reynolds dilatancy can be summarized by a local kinematic relationship, supporting a number of theoretical and numerical approaches [18,19]. Our setup provides a generic and robust way to extract empirical parameters such as limiting densities and characteristic shear scales. In contrast with traditional shearbox tests where the shear zone remains undetermined [8], taking into account the heterogeneity of the flow profile produces well defined material properties.

If the same experiments are repeated with loose sphere piles [see Fig. 4(c)], the material compacts as expected at small strains [20]. However, it rapidly reaches a steady density similar to that previously reported, the values being scattered mostly between 0.59 and 0.6. Our experiments

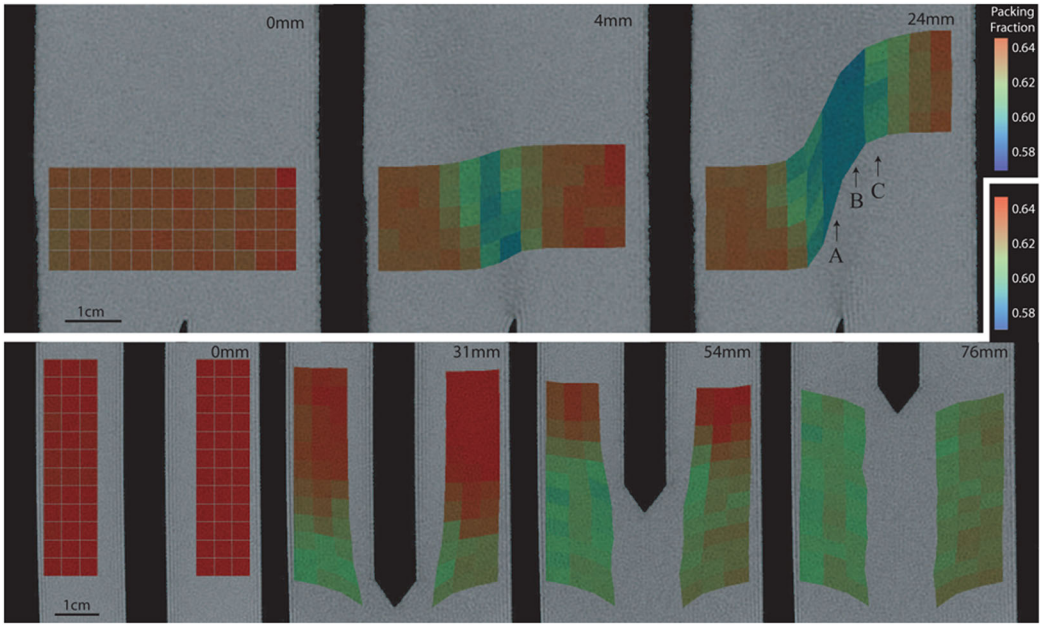

FIG. 2 (color online). Series of radiographs describing the flow and density profiles for a shear flow (top) and gravity driven flow (bottom). Material: monodisperse acrylic spheres, 1 mm in diameter. Numbers on the top right corner of each image indicate the upward displacement of the moving wall. See EPAPS [24] movies Nos. 1 and 2 for the complete sequence of images. Letters designate specific regions discussed in the text and Fig. 4(b).

suggest that the critical state picture [8] is valid, i.e., that a particular packing fraction at which shear can be sustained at constant volume exists and is independent of the initial state and deformation mode.

The generality of this statement is, however, tempered by closer inspection of the data variance. In the gravity flow experiment, nearly all the regions experience a significant increase of the density following the shear-induced expansion (see inset in Fig. 3). This process is known as compaction and corresponds to the intrinsic response of a granular pile to mechanical taps or vibrations [4,21]. Such fluctuations arise in our experiments in the vicinity of flowing regions and cause frequent reorganization of the force network. A similar yet more subtle effect is observed in the forced shear experiments. The packing fraction for a given shear value increases with the distance to the shear band. This is highlighted on Fig. 4(b) but could be seen on all studied systems. This fact again contradicts the existence of a well defined relationship between shear strain and density. Although different regions experience different shear rates, this cannot account for the difference in behavior in a quasistatic experiment. The caution comes in considering the competition of local compaction and dilatancy during shear. The gravity driven experiment, for example, shows that a localized flow can generate stress fluctuations able to cause compaction in remote regions. In the shear band, compaction effects are negligible because it deforms over a time scale where the rest of the sample is mostly static. Away from the shear band, we observe a range of situations where material is being sheared and simultaneously mechanically shaken by the stress fluctuations coming from the shear band. The effect is, as observed, an increase of the resulting density for a given shear strain. The relevance of a critical state has been recently questioned in systems where grain deformation or crushing

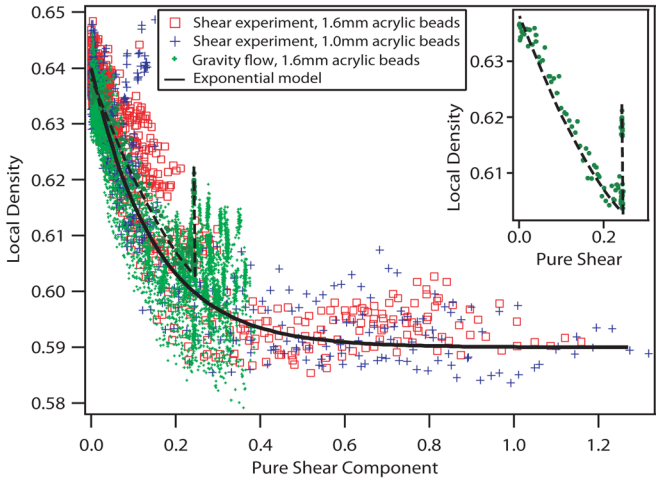

FIG. 3 (color online). Evolution of the local density as a function of the local shear for both flow chambers and various bead sizes; all domains and all times are shown. Piles have been compacted before the experiment starts. The scale for the density (i.e., the value of the absorption length) is measured with $\pm 0.5\%$ accuracy. The inset and dashed line highlight a typical single domain evolution for the gravity flows. Note that these data are unfiltered and show the characteristic noise in the system and measurement.

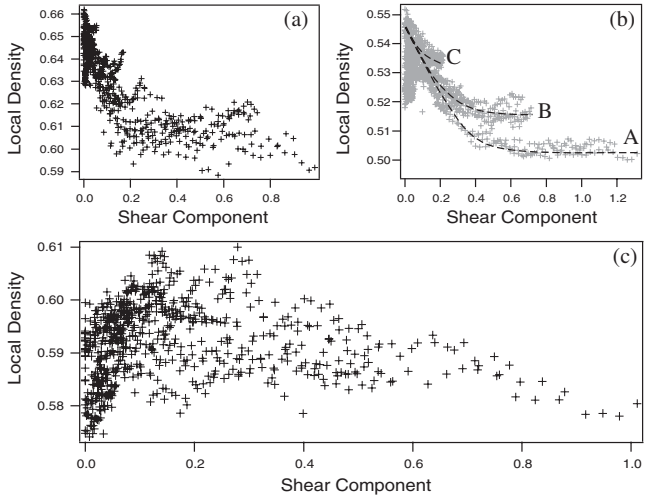

FIG. 4. Local density as a function of the local shear for various materials and initial densities in the shear cell. (a) with monodisperse pasta cylinders, 2 mm in height and diameter. (b) with polydisperse semolina grains, diameters ranging from 0.5 to 1 mm. The dashed lines represent the typical behaviors of the regions *A*, *B*, and *C* defined on Fig. 2. Because of the nature of these materials, absorption coefficients are poorly defined, and the density scale is largely arbitrary. Relative variations are however precise up to 0.1%. (c) Experiment with 1 mm acrylic beads, starting with a loose pile.

is involved [22]. We demonstrate here that even with perfectly rigid grains, the competition between dilatancy and compaction drives the system away from the critical state, even after large shear.

The experimental configuration detailed here offers numerous improvements to the quantification of the relationship between density and flow in granular matter. We demonstrate that, to a first approximation, dilatancy of dense pile can be considered as a kinematic property, with different flow situations providing consistent behavior. This can be applied to a wide range of materials and geometries, up to very large deformations, although the study of nonisotropic grains would require a more complex framework. Interestingly, these experiments also unveil the intricate interplay between Reynold's dilatancy and compaction in complex granular flows. The dilatancy curve measured in shear bands only defines a lower bound to the range of available densities. To characterize the response of the material in other regions, one needs to understand how mechanical fluctuations are generated, propagate, and cause compaction. Although nonlocal elastic fluctuations have been derived from the flow profile in systems like foams [23], such a question represents a major challenge in the context of granular flows where the mechanisms of force propagation and microplasticity are still poorly understood. Nevertheless, this appears to be a key to predict both the density profile and stability of granular flows. The subtle balance between structure relaxation (compaction) and shear-induced disorder (dilatancy) involved in the quasistatic rheology of granular matter deepens further the analogy with jammed and structurally disordered systems such as foams, emulsions, and colloidal glasses.

The authors would like to thank Tomaso Aste, Georges Debrégeas, L. Mahadevan, and Olivier Pouliquen for discussions. T. J. S. gratefully acknowledges the Australian Research Council for support.

*ajk61@cam.ac.uk

[1] H. M. Jaeger, C. H. Liu, and S. R. Nagel, Phys. Rev. Lett. **62**, 40 (1989).
[2] K. To, P-Y Lai, and H. K. Pak, Phys. Rev. Lett. **86**, 71 (2001).
[3] O. Reynolds, Philos. Mag. **20**, 469 (1885).
[4] J. B. Knight, C. G. Fandrich, C. N. Lau, H. M. Jaeger, and S. R. Nagel, Phys. Rev. E **51**, 3957 (1995).
[5] J. Desrues and R. Chambon, Int. J. Solids Struct. **39**, 3757 (2002).
[6] Y. Oyama, Bull. Inst. Phys. Chem. Res. Jpn. Rep. **18**, 600 (1939).
[7] P. Richard, M. Nicodemi, R. Delannay, P. Ribiere, and D. Bideau, Nature Mater. **4**, 121 (2005).
[8] W. Powrie, *Soil Mechanics: Concepts and Applications* (Spon Press, London, 2004), 2nd ed.
[9] Rechenmacher, J. Mech. Phys. Solids **54**, 22 (2006).
[10] K. Sakaie, D. Fenistein, T. J. Carroll, M. van Hecke, and P. Umbanhowar, Europhys. Lett. **84**, 38001 (2008).
[11] J. Desrues, R. Chambon, M. Mokni, and F. Mazerolle, Géotechnique **46**, 529 (1996).
[12] P. Philippe and D. Bideau, Europhys. Lett. **60**, 677 (2002).
[13] A. Kabla, G. Debrégeas, J. M. di Meglio, and T. J. Senden, Europhys. Lett. **71**, 932 (2005).
[14] S. Bergonnier, F. Hild, and S. Roux, J. Strain Anal. Eng. Des. **40**, 185 (2005).
[15] C. Wiebe and G. W. Brodland, J. Biomech. **38**, 2087 (2005).
[16] S. Nemat-Nasser, *Plasticity* (Cambridge University Press, Cambridge, England, 2004).
[17] S. Roux and F. Radjai, *Physics of Dry Granular Media*, edited by H. J. Hermann *et al.* (Kluwer Academic Publishers, Dordrecht, 1998), 229.
[18] J. D. Goddard and A. K. Didwania, Q. J. Mech. Appl. Math. **51**, 15 (1998).
[19] I. F. Collins and B. Muhunthan, Géotechnique **53**, 611 (2003).
[20] M. Nicolas, P. Duru, and O. Pouliquen, Eur. Phys. J. E **3**, 309 (2000).
[21] A. Kabla and G. Debrégeas, Phys. Rev. Lett. **92**, 035501 (2004).
[22] I. F. Collins, B. Muhunthan, A. T. T. Tai, and M. J. Pender, Géotechnique **57**, 437 (2007).
[23] A. Kabla, J. Scheibert, and G. Debrégeas, J. Fluid Mech. **587**, 45 (2007).
[24] See EPAPS Document No. E-PRLTAO-102-071920 for supplementary movies. For more information on EPAPS, see http://www.aip.org/pubservs/epaps.html.